Acta Metallurgica Vol. 29, pp. 1117 to 1130, 1981
Printed in Great Britain.

0001-6160/81/061117-14$02.00/0

A RATIONALISATION OF SHEAR TRANSFORMATIONS IN STEELS

H. K. D. H. BHADESHIA

Department of Metallurgy and Materials Science, University of Cambridge,
Pembroke Street, Cambridge CB2 3QZ, U.K.

(*Received* 2 *July* 1980; *in revised form* 27 *October* 1980)

Abstract—Experimental evidence is provided in support of the theory that Widmanstätten ferrite formation involves the co-operative growth of mutually-accommodating plates. The adjacent plates generally turn out to be similarly oriented, presumably because the simultaneous nucleation of such variants is relatively easy. The mechanism of Widmanstätten ferrite growth is considered to be compatible with an atomic correspondence being maintained for the iron atoms.

It is demonstrated that the concept of ferrite growing with a partial supersaturation with respect to carbon is not tenable, and that the expected growth rates must correspond either to carbon diffusion control or to interface friction control (when the ferrite forms with a full supersaturation). Assuming that this natural distinction between the possible growth rates corresponds to the difference between Widmanstätten ferrite and bainite, thermodynamic conditions are established and tested to enable quantitative distinction between the two products. These conditions are then demonstrated to be consistent with the conventionally accepted morphologies of Widmanstätten ferrite and bainite, and it is shown that the hypothesis that the former involves the equilibrium partitioning of carbon during growth while the latter does not is reasonable in terms of the maximum amounts of transformation permitted for a given set of conditions. An attempt is also made to incorporate nucleation into the overall thermodynamic treatment, and the outcome of all this is that it seems possible to rationalise the shear transformations that occur in steels.

Résumé—Nous apportons des arguments expérimentaux en faveur de la théorie indiquant que la formation de la ferrite de Widmanstätten met en jeu croissance coopérative de plaquettes mutuellement s'accommodant mutuellement. Les plaquettes adjacentes sont généralement orientées de manière semblable, vraisemblablement parce que la germination simultanée de telles variants est relativement facile. Nous pensons que le mécanisme de croissance d'une ferrite de Widmanstätten est compatible avec le maintien d'une correspondance atomique pour les atomes de fer.

Il est demonstré que l'idée de la croissance de ferrite avec partiale sursaturation en carbone n'est pas tenable. Aussi que les vitesses de croissance prévues doivent correspondre au controle par diffusion de carbone ou par la friction de la surface de séparation (quand la ferrite se forme avec totale sursaturation). Avec l'hypothèse que cette distinction naturelle entre les possibles vitesses de croissance correspond avec la différence entre la ferrite Widmanstätten et la bainite, les conditions thermodynamiques sont établies et vérifiées pour pouvoir faire une distinction quantitative entre les deux produits. En suivant, cettes conditions sont démontrées de conformer avec les morphologies conventionnelles de la ferrite Widmanstätten et de la bainite. L'hypothèse que la première condition nécessite la répartition d'equilibre de carbone pendant croissance mais pas pour la deuxieme, est montrée d'etre raisonable en termes des quantités maximums de transformation premises pour un cas particulier. Aussi un effort est fait a incorporer la nucléation dans un total traitement thermodynamique. Le résultat de tout est la possibilité de rationaliser les transformations par poussée qui prends place dans les aciers.

Zusammenfassung—Es werden experimentelle Belege für die Theorie vorgelegt, daß die Bildung des Widmanstätten-Ferrits das kooperative Wachsen sich gegenseitig anpassender Platten einschließt. Benachbarte Platten sind ähnlich orientiert, da die gemeinsame Keimbildung solcher Varianten vermutlich relativ leicht ist. Es wird angenommen, daß der Wachstumsmechanismus des Widmanstätten-Ferrits mit einem entsprechenden Verhalten der Eisenatome auf atomarer Ebene verträglich ist.

Es wird dargelegt, daß das Konzept eines Ferrits, der in einer Übersättigung von Kohlenstoff wächst, nicht haltbar ist, und daß die erwartete Wachstumsrate einer Kontrolle entweder durch Kohlenstoffdiffusion oder durch Grenzflächenreibung entsprechen muß (im Falle der Ferritbildung unter voller Übersättigung). Mit der Annahme, daß diese einfache Unterscheidung zwischen den möglichen Wachstumsraten dem Unterschied zwischen den Widmanstätten-Ferriten und -Bainiten entspricht, werden thermodynamische Bedingungen zur aufgestellt. Diese werden daraufhin geprüft, ob zwischen den beiden Produkten unterschieden werden kann. Anschließend wird gezeigt, daß diese Bedingungen mit den allgemein akzeptierten Morphologien der Widmanstätten-Ferrite und -Bainite verträglich sind und daß die Hypothese, wonach der Ferrit eine Gleichgewichtsaufteilung des Kohlenstoffs während des Wachstums umfaßt, der Bainit jedoch nicht, auf der Grundlage der bei einem gegebenen Satz von Bedingungen maximalen Umwandlung vernünftig ist. Außerdem wird versucht, die Keimbildung in die thermodynamische Behandlung einzubauen; als Ergebnis erscheint es möglich, die in Stählen ablaufenden Scherumwandlungen zu beschreiben.

NOMENCLATURE

P_i, d_i, p_i, m, I	Shape deformation matrix, displacement vector, habit plane, magnitude of the shape strain and identity matrix respectively, for variant (i) of an invariant-plane strain
α, α_w, α_s, γ	Ferrite, Widmanstätten ferrite, supersaturated ferrite, and austenite respectively. Any numerical subscript refers to a particular variant of the lattice correspondence
$x_\alpha^{\alpha\gamma}$, $x_\gamma^{\gamma\alpha}$	Equilibrium carbon concentrations of ferrite and austenite respectively. For alloy steels these are metastable terms when no substitutional-element partitioning occurs
x_γ	General carbon concentration of austenite
$\bar{x}$	Average alloy carbon content
x_m	Maximum level of carbon permitted in ferrite for a specified carbon concentration in the austenite at the interface
T_0	Temperature at which stress-free austenite and stress-free ferrite of the same composition have identical free energies
Ae_3	Temperature corresponding to the $\alpha + \gamma/\gamma$ equilibrium phase boundary for a specified alloy composition and to the metastable phase boundary for no substitutional partitioning.
Ae'_3	Temperature below which elastically-accommodated, singly-tilted plates of α_w can form
B_s, W_s	Temperatures at which bainite and α_w are first observed to form
ΔF^*	Activation energy term of isothermal nucleation theory
F_1, F_2	Stored energy terms for α_w and bainite respectively
F_{st}	Strain energy per unit volume
$\Delta F^{\gamma\rightarrow\gamma_1+\alpha}$	Free energy change accompanying the formation of ferrite which at all times contains an equilibrium carbon content. Any subscript denotes the temperature at which this term is evaluated. For alloy steels this term is computed on the basis of no substitutional-element partitioning
$\Delta F^{\gamma\rightarrow\alpha_s}$	Free energy change accompanying the formation of ferrite of the same composition as austenite. Any subscript denotes the temperature at which this term is evaluated
ΔF_N	Driving force necessary in order to obtain a detectable nucleation rate
σ	Interfacial energy per unit area
R	Gas constant
N	Nucleation rate
ν	Pre-exponential attempt frequency factor of nucleation theory
λ_{1-3}, β	Assumed constants which arise in isothermal martensite nucleation theory
V_α^T	Term indicating the volume fraction of the phase denoted by subscript, obtained by isothermal transformation at temperature T

INTRODUCTION

It is surprising to find that the theory of phase transformations in iron and its alloys still remains unconsolidated and somewhat fragmentary. The lack of continuity is most obvious in the isothermal transformation range, especially where Widmanstätten ferrite forms.

The outstanding feature of this particular reaction is the change in shape, or shape deformation, which reveals itself in the form of a well-defined surface distortion when a pre-polished crystal of austenite is allowed to transform to Widmanstätten ferrite. The surface distortion has been found to correspond to an invariant-plane strain and has a large deviatoric component [1]. Diffusional transformation mechanisms seem incompatible with the existence of such relief [2, 3], whereas if the mechanism is considered to be displacive, then the chemical driving force for transformation is apparently insufficient to account for the strain energy which arises due to the shape change [4]. The difficulty remains even when the carbon atoms are allowed to diffuse ahead of the interface (an atomic correspondence still being maintained for the iron atoms) in order to boost the available driving force.

In an effort to resolve the issue, Bhadeshia [5] recently deduced the existence of a crystallographic degeneracy in the FCC → BCC transformation, and suggested that the degeneracy is compatible with the simultaneous and back-to-back growth of mutually accommodating plates of Widmanstätten ferrite. The degeneracy was shown to be consistent with the adjacent plates being in the same (or nearly the same) crystallographic orientation and having habit plane poles in close proximity, as would be required for the postulated growth mechanism, and to account for the experimental evidence [6] that the tent-like surface relief indicative of mutual accommodation between adjacent plates originates from ferrite regions of 'homogeneous' orientation.

Despite these considerations, it remains to be shown that the theoretically deduced degenerate variants (of the lattice correspondence) do in fact mutually accommodate. It is also necessary to experimentally confirm the general predictions of the theory.

Further difficulties arise if any attempt is made to adopt an overall view of the transformations that occur in steels. While equilibrium carbon partitioning at the α/γ interface is a thermodynamic necessity at high temperatures, it should perhaps be possible for the ferrite to retain increasing fractions of the parent austenite carbon content with successively larger undercoolings (below and Ae_3 temperature), until eventually, at the T_0 temperature, stress-free ferrite *could* form with a full carbon supersaturation. The concept of partial supersaturation for transformations between the Ae_3 and T_0 temperatures not only requires detailed examination, but also needs to be established from a thermodynamic viewpoint.

In discussing the thermodynamics of phase transformations, it is all too easy to forget the role of kinetics—indeed, all attempts to account for the bainite and Widmanstätten ferrite transformations have centered on the balance between the chemical free energy change and the stored energy of the final lattice. However, in the presence of any substantial barrier to nucleation, all such attempts should be invalid.

Finally, a puzzling feature which seems to have gone unnoticed is that the Widmanstätten ferrite, bainite and martensite transformations, all of which result in a shape change, occur in all poorly alloyed steels. However, Widmanstätten ferrite often does not form in medium-alloy and high-carbon steels, and very highly-alloyed steels only transform to martensite. The reasons for such irrationality are not clear and it was the aim of this work to try to resolve this and the other problems mentioned earlier.

EXPERIMENTAL PROCEDURES

Two alloys were used in the present investigation, and the preparation methods used and final compositions (expressed in wt.%) are as follows:

(1) Fe–0.41 C, prepared as a 65 g melt in an argon-arc furnace, swaged down to 3 mm dia. rod.

(2) Fe–4.08 Ni–2.05 Si–0.39 C, prepared as a 20 kg vacuum induction melt, forged and hot rolled to 10 mm dia. rod. A part of this was subsequently homogenised at 1250°C for 3 days while sealed in a quartz tube under a partial pressure of pure argon. After removing 2 mm from the surface, the alloy was further swaged down to 3 mm dia. rod.

The swaging treatments involved successive reductions of diameter in approximately 1 mm steps, and were carried out at ambient temperature in order to avoid oxidation. Both the alloys were prepared from high-purity constituents and thin foil specimens for transmission electron microscopy were prepared as in [7].

For surface relief experiments, specimens were mechanically polished to a $\frac{1}{4}$ μm finish, and sealed in a quartz tube under a partial pressure of high-purity argon before any heat-treatment. The surface relief was imaged using the Normanski Differential Interference technique with a Ziess optical microscope. The tilt sense was determined by through focussing experiments, using grain boundary grooves for reference; when considering combinations of tilts, net upheavals are referred to as 'tent-like', compared with a net depression of the free surface which corresponds to 'vee-shaped' surface relief.

Kikuchi line patterns for orientation analysis were obtained using a Philips EM300 transmission electron microscope operated at 100 kV, and the patterns were analysed according to [8–11].

RESULTS AND DISCUSSION

Part 1: The nature of Widmanstätten ferrite

(i) *Theoretical analysis.* The relationships between independent variants of Widmanstätten ferrite (α_w) were calculated as in [5], but with the experimental α_w/γ orientation relationship, habit plane and shape change data of Watson and McDougall [1]. Bearing in mind that the experimental evidence [6] suggests that adjacent variants are similarly oriented, the aim was to find variants of α_w that are symmetry related and at the same time are consistent with the co-operative growth mode discussed earlier. The back-to-back growth idea makes it necessary to consider only the six variants corresponding to a given close-packed plane in the austenite. The standard variant chosen for the analysis was as follows:

$$(0.5916\ 0.5772\ 0.5628)_\gamma \| (101)_{\alpha_1}$$

$$[0.6984\ \overline{0.7157}\ 0.0001]_\gamma \| [11\bar{1}]_{\alpha_1}$$

Habit plane = $(0.5057\ 0.4523\ 0.7346)_\gamma$

Displacement Vector = $[\overline{0.8670}\ 0.4143\ 0.2770]_\gamma$

The results are presented in Table 1, and it is evident that variants 1 and 6 are in almost identical orientation, while variants 1 and 5 are close to being twin-related.

In order to obtain a ranking in terms of the degree of favourable interaction between pairs of variants, the following procedure was adopted:

(a) The shape deformation matrix P_i (the elements of which are denoted $\{p_{kl}\}_i$) of variant (i) was calculated using the relationship $P_i = I + md_ip_i$, where m is the magnitude of the shape strain, I is the identity matrix and d_i and p_i respectively represent the displacement vector and habit plane of the (i)th variant.

(b) The interaction between variants 1 and i is then represented by

$$\Psi = \frac{\sum_{kl} \{q_{kl}\}_i^2}{\sum_{kl} \{p_{kl}\}_1^2}$$

where $\{q_{kl}\}_i$ are the elements of the matrix

$$Q_i = \{(P_1 + P_i)/2\} - I.$$

The parameter Ψ is so constructed that as the degreee of favourable interaction increases, $\Psi \rightarrow 0$, i.e. the average of the two shape deformations $(P_1 + P_i)/2 \rightarrow$ I. This parameter is only intended to be indicative and does not take account of factors such as the relative volume fractions of the two variants concerned. The results of the analysis are also presented in Table 1.

(ii) *Surface relief experiments and electron microscopy.* Surface relief studies were carried out on the Fe–C alloy after austenitisation of a pre-polished specimen at 1200°C for 2 days followed by isothermal transformation at 700°C for 30 min and air cooling to ambient temperature. Of some 30 prior austenite

Table 1. Calculated crystallographic relationships between Widmanstätten ferrite variants (Note: Sets beyond 1–6 are given only to enable comparison with the experimental results of Table 2)

Designation	Variant description	Axis-angle pair describing the relationship with standard variant	Ψ
(1–2)	$(101)_\alpha \| (\overline{0.5772}\ \ 0.5628\ \ 0.5916)_\gamma$ $[11\bar{1}]_\alpha \| [\overline{0.7157}\ \ 0.0001\ \ 0.6984]_\gamma$	$(\overline{0.7085}\ \ 0.0202\ \ \overline{0.7055})$ 120°	0.274
(1–3)	$(101)_\alpha \| (0.5628\ \ 0.5916\ \ \overline{0.5772})_\gamma$ $[11\bar{1}]_\alpha \| [0.0001\ \ 0.6984\ \ \overline{0.7157}]_\gamma$	$[0.7085\ \ \overline{0.0202}\ \ 0.7055]$ 120°	0.274
(1–4)	$(101)_\alpha \| (\overline{0.5916}\ \ \overline{0.5628}\ \ \overline{0.5772})_\gamma$ $[11\bar{1}]_\alpha \| [\overline{0.6984}\ \ \overline{0.0001}\ \ 0.7157]_\gamma$	$[\overline{0.6371}\ \ 0.4119\ \ 0.0515]$ 180°	0.952
(1–5)	$(101)_\alpha \| (\overline{0.5772}\ \ \overline{0.5916}\ \ \overline{0.5628})_\gamma$ $[11\bar{1}]_\alpha \| [0.7157\ \ \overline{0.6984}\ \ \overline{0.0001}]_\gamma$	$[0.5817\ \ 0.5830\ \ \overline{0.5673}]$ 177.9°	0.180
(1–6)	$(101)_\alpha \| (\overline{0.5628}\ \ \overline{0.5772}\ \ \overline{0.5916})_\gamma$ $[11\bar{1}]_\alpha \| [\overline{0.0001}\ \ 0.7157\ \ \overline{0.6984}]_\gamma$	$[\overline{0.0554}\ \ 0.9949\ \ 0.0842]$ 180°	0.354
(1–9)	$(101)_\alpha \| (0.5772\ \ 0.5916\ \ \overline{0.5628})_\gamma$ $[11\bar{1}]_\alpha \| [\overline{0.7157}\ \ 0.6984\ \ \overline{0.0001}]_\gamma$	$[\overline{0.3476}\ \ \overline{0.4525}\ \ \overline{0.8213}]$ 180°	
(1–10)	$(101)_\alpha \| (\overline{0.5628}\ \ \overline{0.5916}\ \ 0.5772)_\gamma$ $[11\bar{1}]_\alpha \| [\overline{0.0001}\ \ \overline{0.6984}\ \ \overline{0.7157}]_\gamma$	$[0.0503\ \ 0.8657\ \ \overline{0.4981}]$ 119.98°	
(1–13)	$(101)_\alpha \| (0.5916\ \ \overline{0.5628}\ \ \overline{0.5772})_\gamma$ $[11\bar{1}]_\alpha \| [0.6984\ \ \overline{0.0001}\ \ \overline{0.7157}]_\gamma$	$[0.6571\ \ 0.7321\ \ 0.1796]$ 89.99°	

grains examined using interference microscopy (all these contained Widmanstätten ferrite), it was found that all the plates observed exhibited tent-like surface relief, of the type indicated by Watson and McDougall [1]. A few cases of singly tilted plates (henceforth referred to as single plates) were found on isothermally transforming at the lower temperature of 600°C. These observations simply confirm the conclusion reached by Aaronson *et al.* [12], that the occurrence of single plates is rare.

Specimens for electron microscopy were isothermally transformed at 700°C for only 2 min (after austenitisation at 1200°C for 6 h) before water quenching, in order to try and avoid plate impingements. It was intended to confirm, using electron diffraction, that the tent-like relief of Widmanstätten ferrite originates from mutually accommodating variants whose relative orientations are consistent with those indicated in Table 1.

The Widmanstätten ferrite plates were generally found to be associated in groups of two or more adjacent variants in intimate contact, in accord with the proposed back-to-back growth mode.† An example is illustrated in Fig. 1, and the results of eleven such experiments are listed in Table 2. Figure 1 shows a case in which the α_w variants are almost identically disposed (i.e. the 1–6 pair of Table 1).

† In passing, we notice that Kinsman *et al.* [13] reported the dynamic observation of the growth of what appeared to be a single, isolated Widmanstätten ferrite plate, but which was subsequently found to exhibit tent-like relief. Although at the time they interpreted their results differently, in the context of the present work this observation provides powerful support for the *co-operative* growth mode.

Inspection of Table 2 shows that in all but three cases, the adjacent variants correspond to the same close-packed plane in the austenite, as was considered to be necessary for co-operative growth [5]. The exceptions most probably represent the detection of impingement events—it was not always possible (due to the limited amount of electron-transparent area on any specimen) to judge whether the plates under examination were those involved in co-operative growth. Surface relief studies indicated that such impingements can be expected between *sets* of mutually-accommodating pairs (Fig. 2). It should be noted that since the calculations of Table 1 are based on the averaged data of [1], *exact* agreement with the results of Table 2 cannot be expected. For example, the small variations in the relative orientations of the 1–6 pairs of Table 2 probably reflect real variations in the α_w/γ orientation relationship.

A 1–6 counterminous interaction was also observed, as shown in Fig. 3. Such interactions are also

Table 2. Experimentally determined Axis-Angle pairs relating adjacent variants of Widmanstätten ferrite

Variant Set	Axis-Angle Pair	
(1–2)	$[\overline{0.7101}\ \ 0.0171\ \ \overline{0.7039}]$	130°
(1–5)	$[0.5831\ \ 0.5938\ \ \overline{0.5544}]$	175°
(1–5)	$[0.5774\ \ 0.5774\ \ \overline{0.5774}]$	180°
(1–6)	$[0.0003\ \ 0.9999\ \ \overline{0.0027}]$	180°
(1–6)	$(\overline{0.0355}\ \ \overline{0.9993}\ \ \overline{0.0129})$	165°
(1–6)	$[\overline{0.0319}\ \ \overline{0.9919}\ \ \overline{0.1232}]$	178°
(1–6)	$[\overline{0.0210}\ \ 0.9995\ \ 0.0256]$	179°
(1–6)	$[\overline{0.0001}\ \ \overline{0.9999}\ \ \overline{0.0002}]$	180°
(1–9)	$[\overline{0.2139}\ \ \overline{0.5041}\ \ \overline{0.8368}]$	173°
(1–10)	$[\overline{0.2296}\ \ \overline{0.8821}\ \ \overline{0.4113}]$	113°
(1–13)	$[\overline{0.5093}\ \ \overline{0.8260}\ \ \overline{0.2413}]$	91°

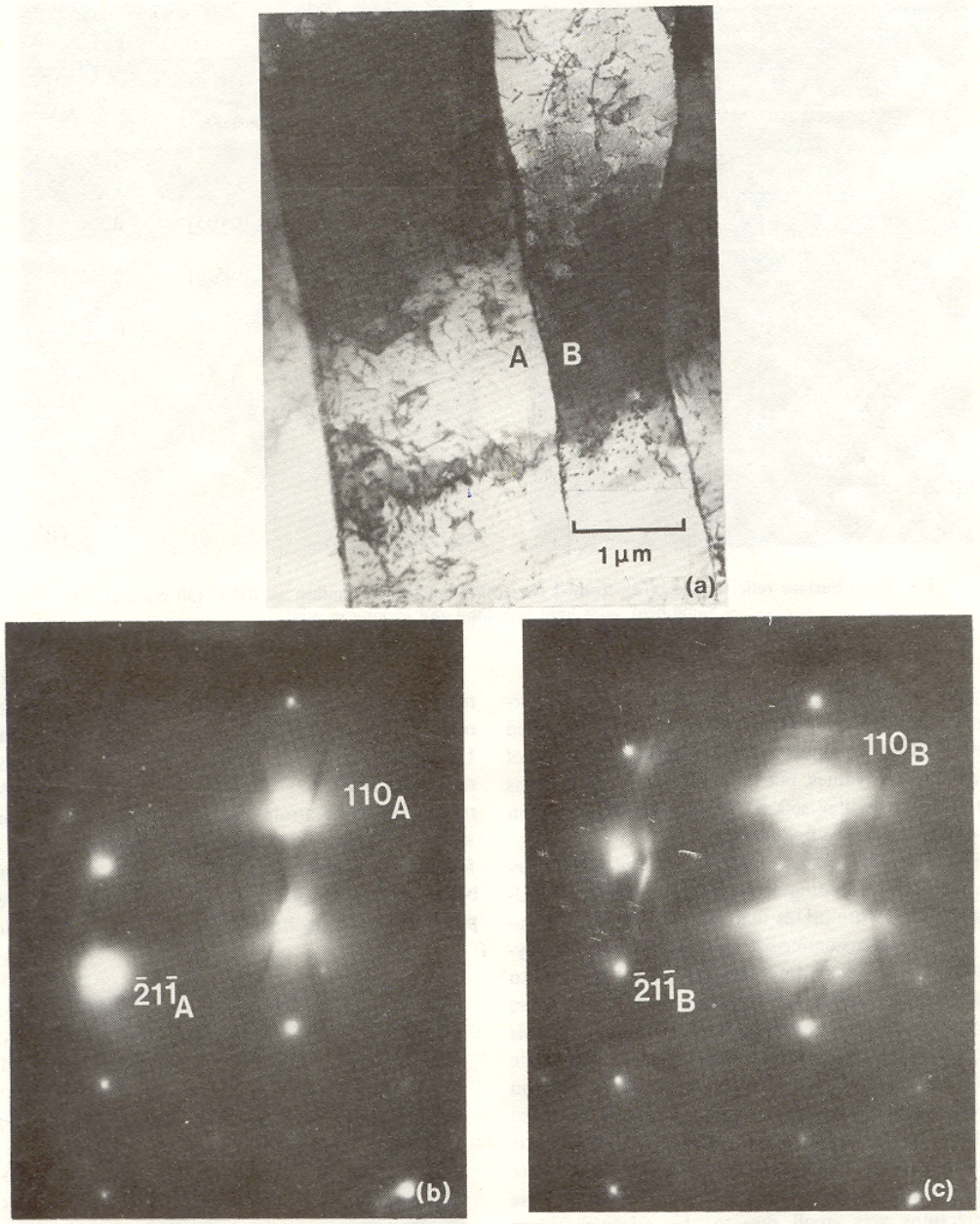

Fig. 1. Electron micrograph and corresponding diffraction patterns from a pair of back-to-back α_w plates in almost identical orientation in space (i.e. a 1–6 pair, related by a rotation of 180° about $[\langle 0.0003\ 0.9999\ 0.0027\rangle]_\alpha$ axis). The central bright spots are Fe_2O_3 surface oxide reflections.

expected to lead to strain energy reduction, and are a feature of many shear transformations [14, 18]. Dynamic observations [18] on a non-ferrous alloy have indicated that such pairs of plates grow outwards from their common junction, and get thinner away from this 'interaction zone', as would be thought likely from strain energy considerations.

Judging from the data of Table 2, it would appear that the 1–5 and 1–6 pairs are the most favourable, with the latter dominating. The occurrence of the 1–5 pair is not surprising due to the associated low Ψ value (Table 1). However, the frequency of 1–6 pairs is more difficult to understand since Ψ_{1-6} is greater than Ψ_{1-2}, Ψ_{1-3} and Ψ_{1-5}, and yet the data of Table 2 indicates that 1–2 and 1–3 sets rarely form while the probability of the formation of the 1–5 pair is lower than that of the 1–6 pair. However, the results can be rationalised if it is considered that the co-operative nucleation of variants is easiest when the variants concerned are similarly oriented. Such a criterion

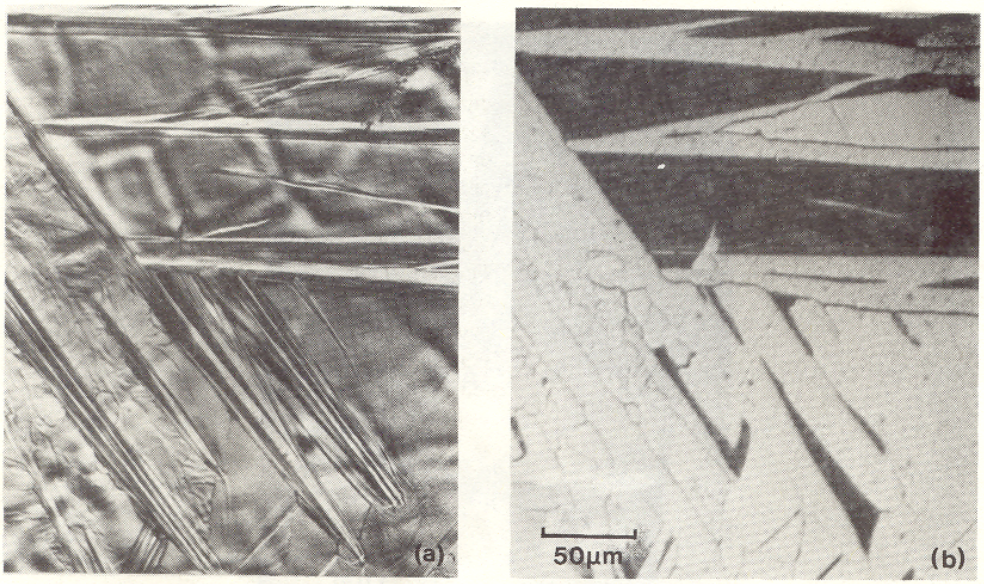

Fig. 2. (a) Surface relief image of α_w formed by isothermal transformation at 700°C (30 minutes). (b) Same field, after light polishing and etching in nital.

would favour the formation of 1–6 pairs. The apparently more frequent occurrence of 1–5 pairs compared with 1–2 or 1–3 pairs could be understood in terms of the relative Ψ values, but the number of observations on these particular sets is insufficient to be certain about their relative frequencies.

(iii) *Thermodynamics of Widmanstätten ferrite formation.* The preceding analysis indicates that Widmanstätten ferrite plates tend to grow in a co-operative, mutually-accommodating manner. Since singly-tilted plates *are* sometimes observed [1], it is useful to examine the feasibility of forming such plates when they are elastically accommodated. Any such analysis requires an estimate of the plate aspect ratio; plate thickness measurements were carried out on electron micrographs, and were stereographically resolved normal to the habit plane. The habit plane was assumed to be $\{110\}_\alpha$, and foil thickness effects were taken into account although the magnitude of these corrections was small due to the relatively large dimensions of the plates involved. The average thickness from 14 such measurements was found to be 1.4×10^{-6} m (standard deviation $s = 7.8 \times 10^{-7}$ m). Foil thickness limitations prevented the simultaneous measurements of plate lengths, but from 90 separate measurements† the mean length was found to be 1.56×10^{-4} m ($s = 7 \times 10^{-5}$ m), giving an aspect ratio of 9×10^{-3} ($s = 6.4 \times 10^{-3}$). Using the latter result, the shape strain data of [1] and elastic constants from [4], the strain energy per unit volume of ferrite was calculated as in [20]. The temperature below which elastically-accommodated, singly-tilted plates of Widmanstätten ferrite can form (i.e. the Ae'_3

Fig. 3. Electron micrograph illustrating a 1–6 counterminous interaction.

† The 90 length measurements taken from random sections were related to the true average length $\bar{L}$ by the equation [19] $\bar{L} = \pi/2\bar{Z}$, where $\bar{Z}$ is the mean of the reciprocal of the lengths of the line segments observed in the sectioning plane. This treatment uses the assumption that the particles are circular discs and is expected to somewhat underestimate the length since α_w plates are in fact laths [1]. It should be noted that the value of $\bar{L}$ obtained using the above equation was found to be only 10% bigger than that obtained simply by taking the mean of all the measurements taken from random sections.

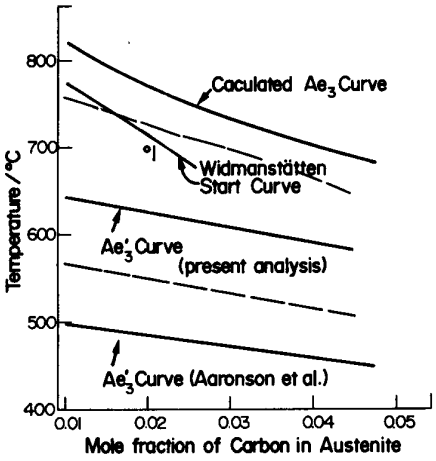

Fig. 4. Calculated Ae_3 and Ae'_3 curves, as discussed in the text. The open circle and the vertical bar correspond to the present experiments and those of Watson and McDougall, respectively. The dashed lines refer to Ae'_3 calculations using values of the aspect ratio differing by one standard deviation about the mean value.

temperature) was obtained as a function of carbon content by balancing the strain energy against the chemical free energy change accompanying the formation of ferrite with an equilibrium carbon content (i.e. $\Delta F^{\gamma\rightarrow\gamma_1+\alpha}$). The latter was calculated using the formalisms and data of [21–25].

The results are plotted in Fig. 4 along with the earlier calculations Aaronson *et al.* [4]. The difference between the two sets of results arises because the aspect ratio used in the calculations of [4] was simply estimated from optical micrographs of randomly sectioned specimens. It it clear that somewhat better agreement is obtained between the calculated Ae'_3 curve and the curve representing the highest temperature at which Widmanstätten ferrite is observed to form (i.e. the W_s curve). It is believed that a number of factors can explain the remaining discrepancy; the calculations presented in Fig. 4 are based on elastically-accommodated plates whereas experiment [1, 26] and theory [27] suggest that considerable plastic deformation accompanies transformation. In addition, strain interactions and the presence of free surfaces have not been taken into account.

Part II: The link between Widmanstätten ferrite and bainite

(i) *The nucleation problem.* As mentioned in the introduction, it is essential to obtain at least an indication of the amount of driving force (ΔF_N) necessary in order to ensure a detectable nucleation rate for transformation. Unfortunately, current nucleation theories are not sufficiently established to enable the calculation of this quantity from first principles. In the present work an attempt is made to bypass this difficulty by resorting to experimental data.

It is well known that in low-alloy steels a pronounced bay appears in the time-temperature-transformation (TTT) curves; this bay is usually identified with the bainite start (B_s) temperature, although it does not seem to have been demonstrated to correspond to the beginning of *bainite* formation. However, in general it may be assumed that whenever the bay is pronounced, as in low-alloy steels, the 'B_s' temperature corresponds to the temperature at which ferrite first forms with a shape change (this is true for the Fe-Mn-Si-C steel examined in [7]). Certainly, the continuity of W_s and B_s with increasing carbon or alloy content has often been assumed in various treatments [e.g. 28]. Furthermore, it will become evident later that the assumption is justified, not only on the basis of experimental evidence on an Fe-Ni-Si-C steel, but also because the outcome of the analysis will indicate that the nucleation of α_w and of bainite is similar.

For the purposes of the present analysis, it is also assumed that the B_s temperature corresponds to the temperature where a detectable nucleation rate (for ferrite formation with a shape change) first becomes possible. This assumption is consistent with the established theory of 'C' curve kinetics and with the work of [7]; this interpretation is also in agreement with the experiments of Steven and Haynes [29] which provide a rich source of painstakingly evaluated data on the variation of the 'B_s' temperature as a function of alloy composition. This data was used to calculate ΔF_N under two circumstances—that in which the ferrite forms with the parent austenite carbon content ($\Delta F^{\gamma\rightarrow\alpha_s}$), and that when ferrite has an equilibrium carbon content ($\Delta F^{\gamma\rightarrow\gamma_1+\alpha}$), with the excess being rejected at the transformation interface; substitutional-element partitioning was not allowed in either case. The calculation procedures are given elsewhere [30, Appendix 1], and are not repeated here, but it is expected that they refer to grain boundary nucleation since both bainite and Widmanstätten ferrite inevitably nucleate at such sites.

The results are plotted in Fig. 5 from which it seems that the formation of a nucleus with the equilibrium carbon content is the true circumstance; the alternative hypothesis would lead to nucleation against a positive driving force for a few of the steels examined. Intuitively, the formation of a nucleus with an equilibrium carbon content seems more reasonable (irrespective of the carbon content of the ferrite at the growth stage) when we consider (as did Volmer [31]) that the thermally activated development of an embryo to the critical nucleus size occurs through a large number of small scale fluctuations, rather than a sudden large fluctuation. Under such circumstances the rejection of the few carbon atoms that would be expected within the critical nucleus volume should be readily feasible.

From Fig. 5a it is evident that *all* the reported 'B_s' temperatures cannot correspond to the formation of *bainite*, since in some cases there is insufficient driving force to account for growth involving the formation of fully supersaturated ferrite. On the other hand, the

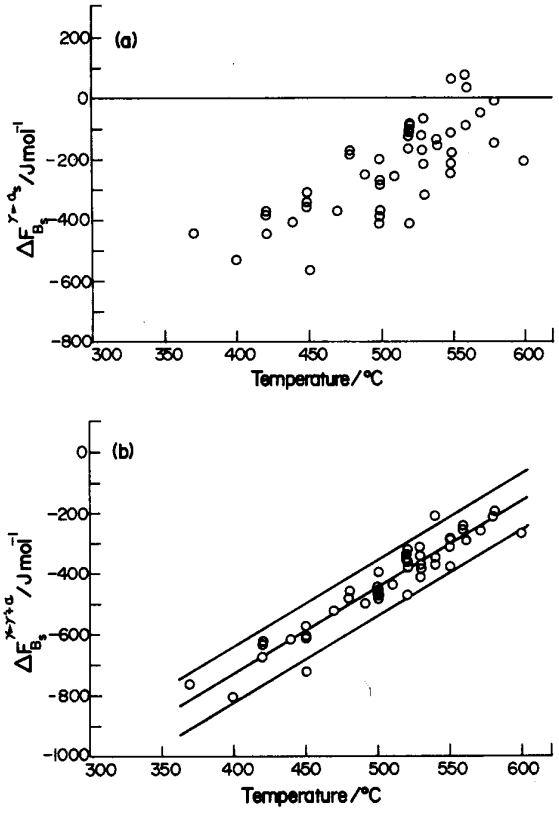

Fig. 5. Curves representing the volume free energy change necessary in order to obtain a detectable nucleation rate for ferrite forming by shear. (a) The case when the volume free energy change is calculated on the basis that the ferrite nucleus inherits the parent austenite carbon content. (b) The case when the volume free energy change is calculated on the basis that the ferrite nucleus at all times contains only an equilibrium carbon content. The lines bounding the regression line are vertically spaced at distances equivalent to two standard errors of the estimate from the regression line.

data of Fig. 5b closely corresponds to a *single* straight line. Since the so-called B_s temperature really seems to correspond to the first temperature at which the nucleation of ferrite (which exhibits an invariant-plane strain relief) first becomes possible, the results of Fig. 5 suggest that the nucleation of both Widmanstätten ferrite and bainite is similar and involves the equilibrium partitioning of carbon. As the growth of bainite involves the full supersaturation of carbon [30], it is possible that the nucleus can develop into either α_w or bainite, depending on whether the driving force available for *growth* beyond the critical nucleus size is sufficient to allow the development of full supersaturation. The free energy available for growth is expected to be enhanced beyond the critical size due to the decreasing contribution of interfacial energy per unit volume, with increasing size.

For many of the steels involved, there is considerable free energy available at the 'B_s' temperature to account for full supersaturation (Fig. 5a). It is in these cases that the nuclei can develop into bainite; otherwise bainite can only form at higher undercoolings than indicated by the 'B_s' temperature. These aspects will be quantitatively developed in a later section of this paper.

Considering now the form of Fig. 5b, the variation of ΔF_N with T may be understood if it is accepted that the method involved the calculation of the free energy change ($\Delta F_{B_s}^{\gamma-\gamma_1+\alpha}$) necessary to give a certain constant, detectable nucleation rate (N), irrespective of the steel used. Through nucleation theory,

$$N \propto \nu \exp(-\Delta F^*/RT) \tag{1}$$

where

ν = pre-exponential attempt frequency factor
ΔF^* = activation barrier
R = gas constant

$$-\Delta F^* \propto RT \ln\left(\frac{N}{\nu}\right)$$

or

$$-\Delta F^* \propto \beta T \tag{2}$$

where

$$\beta = R \ln\left(\frac{N}{\nu}\right).$$

It follows that β is a constant since N is a constant irrespective of the steel used (we only analyse data at B_s). β is expected to be negative, since the nucleation rate must be less than the attempt frequency. Now† [Olson and Cohen, 32]:

$$\Delta F^* = \lambda_1 \Delta F_{B_s}^{\gamma \rightarrow \gamma_1 + \alpha} + \lambda_1 F_{St} + \lambda_2 \sigma + \lambda_3 \qquad (3)$$

where λ_{1-3} are assumed constant characteristics of the lattice and of the nucleus, F_{St} is the strain energy per unit volume of the nucleus and σ is the interfacial energy per unit area. From equations (2) and (3), it follows that

$$-\lambda_1 |\Delta F_{B_s}^{\gamma \rightarrow \gamma_1 + \alpha}| \propto |\beta| T - \lambda_1 |F_{St}| - \lambda_2 |\sigma| - \lambda_3$$

so that $-|\Delta F_{B_s}^{\gamma \rightarrow \gamma_1 + \alpha}| \propto T$, as observed in Fig 5b. Henceforth the curve of Fig. 5b will be assumed to be a *univeral curve* expressing ΔF_N as a function of T, so that a detectable nucleation rate should only be possible in any particular steel if $|\Delta F^{\gamma \rightarrow \gamma_1 + \alpha}|$ for that steel exceeds $|\Delta F_N|$ at the temperature concerned. This seems justified in view of the nature of the analysis and the wide range of steels accounted for in the calculations.

(ii) *Partial supersaturation.* Bainite has often been considered to form with only a partial supersaturation with respect to carbon [33, 34]. All experimental measurements of the carbon content of bainitic ferrite are consistent with some partitioning during growth, but can also be explained in terms of the *subsequent* rejection of carbon from an initially fully saturated ferrite lattice. As Kinsman and Aaronson have pointed out, the latter process could occur in a matter of milliseconds ([35] but their calculations are in error by a factor of π).

Referring to Fig. 6, x_m represents the maximum permitted level of carbon supersaturation in ferrite which precipitates from austenite of composition $\bar{x}$. It is evident that growth involving partial supersaturation (such as that indicated by the interface tie-line $x_m - \bar{x}$) would be *unstable* to perturbations in the interface compositions, and the assembly should irreversibly cascade towards the equilibrium partitioning of carbon (tie-line $x_\alpha^{\alpha\gamma} - x_\gamma^{\gamma\alpha}$), especially since the mobility of carbon in iron is high. Experimental evidence supports this conclusion since the growth of Widmanstätten ferrite seems consistent with the equilibrium partitioning of carbon, irrespective of the degree of undercooling below the $\alpha + \gamma/\gamma$ phase boundary [28].

Hence it is believed that only two types of ferrite growth need to be considered—one involving carbon diffusion control (with equilibrium partitioning of carbon) and the other involving a full carbon supersaturation with interfacial friction control, but in essence martensitic. Clearly, the transition between these growth modes should be 'sharp'.

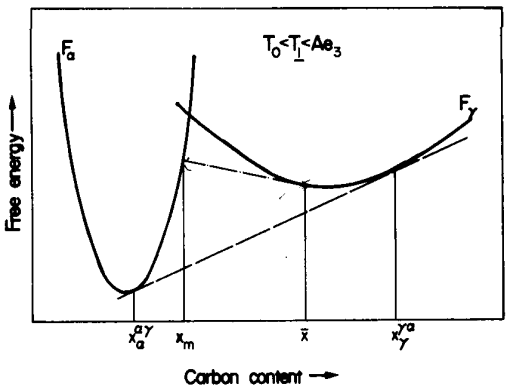

Fig. 6. Schematic γ and α free energy curves illustrating the unstable nature of any assembly in which the ferrite forms with only a partial supersaturation.

(iii) *The transition from Widmanstätten ferrite to bainite.* The concepts developed earlier may be thermodynamically expressed as follows:

Letting F_1 = Stored energy per mole of Widmanstätten α

F_2 = Stored energy per mole of bainitic α.

Widmanstätten ferrite will then form below the Ae_3 temperature when

$$|\Delta F^{\gamma \rightarrow \gamma_1 + \alpha}| > F_1 \qquad (a)$$

$$|\Delta F^{\gamma \rightarrow \gamma_1 + \alpha}| > \Delta F_N. \qquad (b)$$

However, since the driving force necessary for a detectable amount of nucleation (i.e. ΔF_N) should always be greater than that necessary to sustain growth, ΔF_N will always exceed F_1 and condition (a) becomes redundant.

Bainite will form below the T_0 temperature when

$$|\Delta F^{\gamma \rightarrow \alpha_s}| > F_2 \qquad (c)$$

and

$$|\Delta F^{\gamma \rightarrow \gamma_1 + \alpha}| > \Delta F_N. \qquad (d)$$

However, in any steel where the Widmanstätten ferrite transformation precedes bainite formation, condition (d) will probably be redundant. This is because $\Delta F^{\gamma \rightarrow \gamma_1 + \alpha}$ varies approximately linearly and monotonically with temperature, so that once (a) has been satisfied, the further lowering of temperature will not in general lead to a violation of (d). F_1 was calculated from Fig. 4 to be approx. 50 J/mol by evaluating $\Delta F_{W_s}^{\gamma \rightarrow \gamma_1 + \alpha}$. An Fe–Ni–Si–C steel was used to test whether the above definitions are consistent with the observed morphologies of ferrite and to determine F_2. Calculations had indicated that this steel should have a bigger temperature range in which ferrite is able to form (with a shape change) compared with the Fe–

† Here, in accordance with the theory of isothermal nucleation of martensite [32], a linear dependence of activation energy on the chemical driving force is assumed.

Mn–Si–C steel used in [30]. At the same time, the highest temperatures of this range did not seem to be high enough to allow interference from diffusional transformations. In addition, the silicon was anticipated to considerably retard the pearlite transformation and to prevent the precipitation of cementite from austenite.

After austensitising at 1080°C for 15 min, a series of specimens were isothermally transformed at temperatures ranging between 350°C and 650°C before finally quenching into water. Surface relief experiments were also carried out for selected transformation conditions. The results are presented in Figs 7 and 8. It was found that transformation at a temperature between 470°C and 550°C (Fig. 7a) resulted in the formation of isolated, apparently homogeneous plates with the classical Widmanstätten ferrite thin-wedge morphology. Electron microscopy confirmed that the plates observed optically corresponded to pairs of adjacent variants in almost the same crystallographic orientation, again consistent with the nature of Widmanstätten ferrite. Similarly, surface relief experiments established the classical tent-like relief of adjacent mutually-accommodating variants (Fig. 7b).

On the other hand, transformation at temperatures below 470°C (only a very small quantity of sub-unit type morphology was observed at 470°C, the majority of the transformation product being α_w, as illustrated in Fig. 7) resulted in sheaves of subunits (Fig. 8a) with a morphology and size identical to that reported by Bhadeshia and Edmonds [30]. The sub-units in any given sheaf had *identical* tilts (Fig. 8b), although accommodation between adjacent sheaves sometimes led to an apparent tent-like relief on a more macroscopic scale.

Isothermal transformation at 470°C (for 2 h) until reaction termination gave $V_\alpha = 0.79$, where V_α is the volume fraction of ferrite determined by quantitative metallography. On the basis that the ferrite forms with an equilibrium carbon content, $V_{\alpha_w}^{470}$ is expected

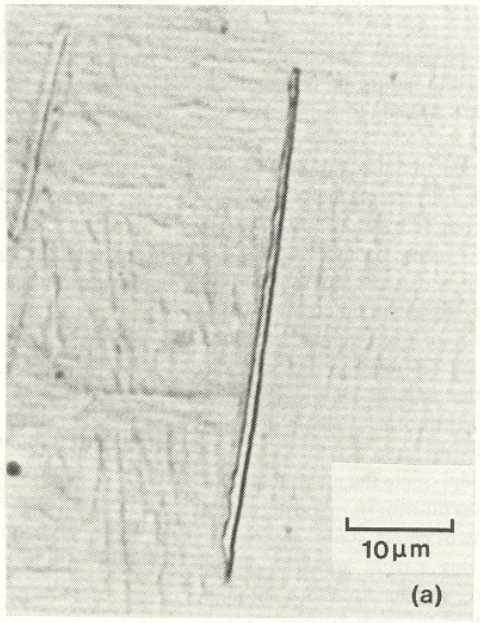

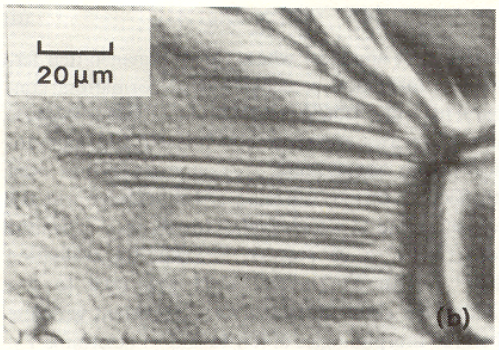

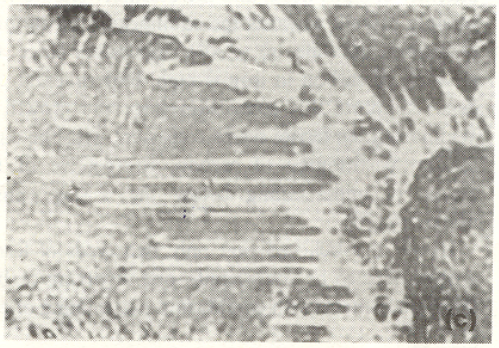

Fig. 7. Fe-Ni-Si-C steel. (a) Wedge shaped α_w obtained by partial isothermal transformation at 470°C for 60 s. (b) The tent-like surface relief image of α_w (isothermally transformed at 510°C for 15 minutes and air-cooled). (c) Same field as in (b), after light polishing and etching in nital.

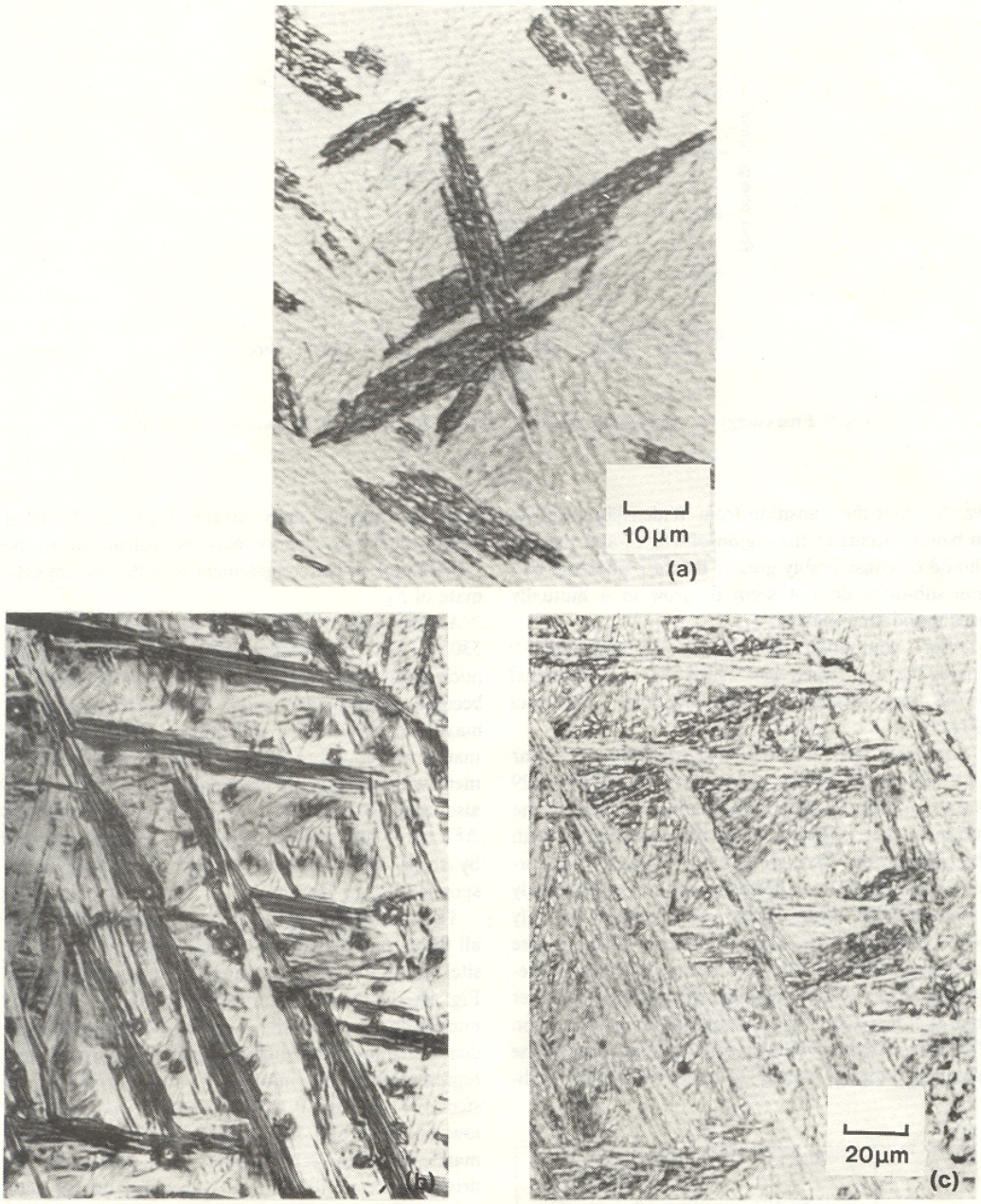

Fig. 8. Fe-Ni-Si-C steel. (a) Optical micrograph showing bainite sheaf formation. The specimen was isothermally transformed at 412°C before water quenching. (b) Surface relief image showing identically tilted sub-units within a bainite sheaf (isothermally transformed at 350°C for 30 minutes and air cooled). (c) same field as in (b), after light polishing and etching in nital.

to be 0.83, while the expected amount of bainite (initially supersaturated) was calculated to be $V_{\gamma_s}^{470} = 0.47$. These quantities were calculated as in [30], and do not take account of strain energy, but the results clearly support the conclusion that α_w forms at temperatures above ~470°C. Furthermore, isothermal transformation (until reaction termination) at 340°C to sheaves of bainite gave $V_{\gamma}^{340} = 0.71$, in agreement with that expected for supersaturated ferrite formation i.e. $V_{\gamma_s}^{340} = 0.70$), but well below the predicted quantity of Widmanstätten ferrite ($V_{\gamma_w}^{340} = 0.89$). It should be noted that consistent with the earlier discussion, the quantity of Widmanstätten ferrite formed at 470°C indicates equilibrium partitioning of carbon, despite the high undercooling below the Ae_3 temperature. From the above results it

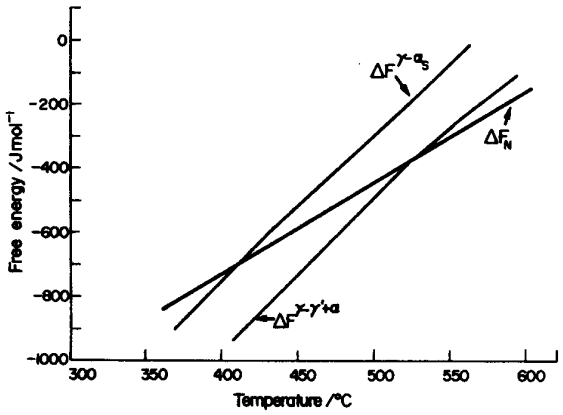

Fig. 9. Free energy vs. temperature curves for the Fe–Ni–Si–C steel, as discussed in the text.

was felt that the transition from Widenstätten ferrite to bainite occurs in the region of 470°C, and that F_2 should be considerably greater than F_1 since the bainite sub-units do not seem to *grow* in a mutually accommodating manner.

After computing the $\Delta F^{\gamma\rightarrow\gamma_1+\alpha}$ and $\Delta F^{\gamma-\alpha_s}$ curves for the Fe–Ni–Si–C steel, F_2 was estimated to be about 400 J/mol since $\Delta F^{\gamma\rightarrow\alpha_s}_{470} \simeq -400$ J/mol (Fig. 9).

Srinivasan and Wayman [36] reported the shear and dilatational strains of lower bainite to be 0.129 and 0.014 respectively. Taking the aspect ratio of the sub-units they observed to be 0.014 (consistent with the micrographs they present, but probably inaccurate due to the reasons given in part 1), the elastically accommodated strain energy would amount to only ~90 J/mol. However, Srinivasan and Wayman were careful to point out that their measurements may reflect an *apparent* shape change which should be lower than that associated with a single sub-unit. Based on the fitting of experimental crystallographic data to the phenomenological theory of martensite, they indicated an expected shape strain of about 0.24, from which the strain energy may be calculated to be ~300 J/mol, in better agreement with the present estimate of F_2.

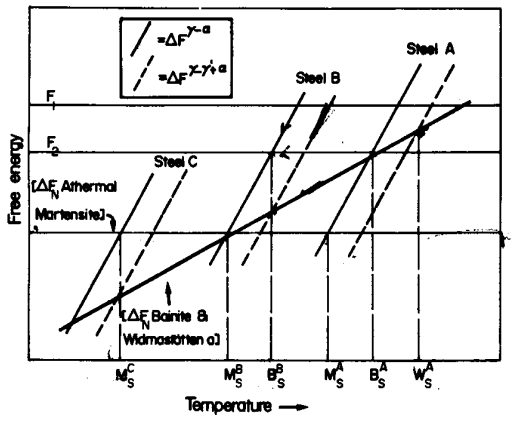

Fig. 10. Schematic free energy curves illustrating why all three shear transformations need not occur in all steels.

Another observation from Fig. 9 is that at about 530°C, $|\Delta F^{\gamma\rightarrow\gamma+\alpha}|$ becomes less than ΔF_N, so that the nucleation rate of ferrite forming by shear ought to become undetectably small. Metallographically the maximum temperature of Widmanstätten ferrite formation was found to be about 590°C, in good agreement with the theoretical deduction, and this would also seem to justify the earlier assumption that the ΔF_N curve refers to the nucleation of ferrite forming by shear, irrespective of whether this ferrite corresponds to α_w or bainite.

The above concepts can in principle explain why all three transformations (i.e. α_w, bainite and martensite) do not necessarily occur in all steels. Referring to Fig. 10, the driving force necessary for the *athermal* nucleation of martensite is indicated to be independent of temperature; such behaviour is approximately representative of martensitic transformation in steels [37]. In Fig. 10, steels A, B and C correspond to low, medium and high-alloy steels respectively, as manifested in the relative amounts of transformation driving force available at any specified temperature. In steel B when $|\Delta F^{\gamma\rightarrow\gamma_1+\alpha}|$ becomes greater than ΔF_N, $|\Delta F^{\gamma-\alpha_s}|$ also exceeds F_2 so that the first shear transformation to occur would lead to bainite formation. Similarly steel C is expected to exhibit only martensite.

SUMMARY AND CONCLUSIONS

It appears that Widmanstätten ferrite formation generally involves the co-operative growth of mutually-accommodating crystallographic variants which are usually (although not always) similarly oriented in space. The thin-wedge morphology of Widmanstätten ferrite can then be understood in terms of the different habit plane poles of the back-to-back plates concerned. Thermodynamically, Widmanstätten ferrite

can only form with an equilibrium carbon content, so that the growth rate is carbon diffusion controlled; however, an atomic correspondence is still maintained with respect to the iron atoms, in agreement with the observed shape change effects.

On the other hand, bainite has to be classified as a martensitic transformation, since its growth seems to involve a full carbon supersaturation. The macroscopic isothermal characteristics normally associated with bainite can be attributed to the operation of the sub-unit mechanism discussed in [30]; this mechanism is really only a manifestation of the relatively low driving force available, so that the motion of the interface is soon terminated by an accumulating friction stress. Bainite seems to be admirably suited for the achievement of a maximum free energy release rate; the growth of the initial sub-unit would be fast, only limited by lattice friction, and at its termination it is able to partition its excess carbon into the residual austenite, thus achieving a further free energy decrement. Although the *final* structure would in *essence* be similar to that of Widmanstätten ferrite, the stored energy of bainite is expected to be considerably higher because of the absence of favourable strain interactions *within* the sheaves of sub-units. Finally, the nucleation of bainite seems to be similar to that of Widmanstätten ferrite, and this may explain the significant crystallographic differences between martensite and bainite.

Although the lower bainite transformation has not been previously considered in the text, it is thought that lower bainite is only a morphological variant of bainite in general. Lower bainite sub-units have been shown to be capable of growing to the size of the austenite grains [7], consistent with the greater available driving force due to the higher undercooling below the T_0 temperature. Because of this higher reaction driving force, the sub-units are capable of rapid adjacent nucleation [7, 38], thus hindering the post-bainitic diffusion of carbon into the residual austenite, and thereby allowing time for the precipitation of carbides with the bainitic ferrite.

Acknowledgements—I am grateful to the Science Research Council for the provision of a research fellowship, and to Professor R. W. K. Honeycombe for the provision of laboratory facilities. I should also like to express my sincere gratitude to Professors J. W. Christian and R. W. K. Honeycombe for very helpful discussions on this work.

REFERENCES

1. J. D. Watson and P. G. McDougall, *Acta metall.* **21**, 961 (1973).
2. J. W. Christian, *Monogr. Ser. Inst. Metals* **33**, 129 (1969).
3. J. S. Bowles and C. M. Wayman, *Acta metall.* **27**, 833 (1979).
4. H. I. Aaronson, M. G. Hall, D. M. Barnett and K. R. Kinsman, *Scripta metall.* **9**, 705 (1975).
5. H. K. D. H. Bhadeshia, *Scripta metall.* **14**, 821 (1980).
6. K. R. Kinsman, R. H. Richman and J. D. Verhoeven, *Mater. Sci. Symp. Abst.* ASM, 41 (1974).
7. H. K. D. H. Bhadeshia and D. V. Edmonds, *Metall. Trans.* A **10**, 895 (1979).
8. P. H. Pumphrey and K. M. Bowkett, *Physica status solidi* (a) **2**, 339 (1970).
9. P. H. Pumphrey and K. M. Bowkett, *Phys. status solidi* (a), **5**, K155 (1971).
10. P. H. Pumphrey and K. M. Bowkett, *Phys. status solidi* (a), **3**, 375 (1970).
11. G. Thomas, *Diffraction and Imaging Techniques in Material Science* (Edited by S. Amelinckx, R. Gevers and J. Van Landuyt), p. 399. North Holland, Amsterdam (1978).
12. K. R. Kinsman, E. Eichen and H. I. Aaronson, *Metall. Trans. A* **6**, 303 (1975).
13. K. R. Kinsman, E. Eichen and H. I. Aaronson, Unpublished research, referred to in a review by H. I. Aaronson, C. Laird and K. R. Kinsman, *Phase Transformations*, ASM, Metals Park, Ohio, 383 (1968).
14. P. D. Southwick and R. W. K. Honeycombe, *Proceedings of the International Conference on Martensitic Transformations*, ICOMAT, Boston, p. 189, Fig. 26 (1979).
15. H. Okamoto, M. Oka and I. Tamura, *Trans. Japan Inst. Metals* **19**, 674 (1978).
16. I. Tamura, Proceedings of the First J.I.M. International Symposium on *New Aspects of Martensitic Transformation*, Kobe, Japan, 59 (1976).
17. H. Okamoto, M. Oka and I. Tamura, *ibid.* 47 (1976).
18. M. M. Kostic, E. B. Hawbolt and L. C. Brown, *Metall. Trans. A* **7**, 1643 (1976).
19. R. T. DeHoff, *Quantitative Microscopy* (Edited by R. T. DeHoff and F. N. Rhines), p. 140. McGraw-Hill, New York (1968).
20. J. W. Christian, *The Theory of Transformations in Metals and Alloys*, Part I, 2nd edn, p. 466. Pergamon Press, Oxford (1975).
21. J. R. Lacher, *Proc. Camb. phil. Soc. math. phys. Sci.* **33**, 518 (1937).
22. R. H. Fowler and E. A. Guggenhiem, *Statistical Thermodynamics*, Cambridge University Press, New York, 1939.
23. H. I. Aaronson, H. A. Domian and G. M. Pound, *Trans. Metall. Soc.* A.I.M.E. **236**, 753 (1966).
24. G. J. Shiflet, J. R. Bradley and H. I. Aaronson, *Metall. Trans. A* **9**, 999 (1978).
25. J. A. Lobo and G. H. Geiger, *Metall. Trans. A* **7**, 1347 (1976).
26. H. M. Clark and C. M. Wayman, *Phase Transformations*, ASM, Metals Park, Ohio, 59 (1968).
27. H. I. Aaronson, Unpublished research referred to in *Scripta metall.* **14**, 825 (1980).
28. M. Hillert, Report on *The Growth of Ferrite, Bainite and Martensite*, Swedish Institute for Metal Research, Stockholm, 1960; also, *Metall. trans. A* **6**, 5 (1975).
29. W. Steven and A. G. Haynes, *J. Iron Steel Inst.* **183**, 349 (1956).
30. H. K. D. H. Bhadeshia and D. V. Edmonds, *Acta Metall.* **28**, 1265 (1980).
31. M. Volmer, *Kinetik der Phasenbildung*, Steinkoff, Dresden (1939) referred to in [20].
32. G. B. Olson and M. Cohen, *Metall. Trans. A* **7**, 1915 (1976); C. L. Magee, *Phase Transformations*, ASM, Metals Park, Ohio, 115 (1970); V. Raghavan and M. Cohen, *Metall. Trans.* **2**, 2409 (1971).
33. J. W. Christian, *The Theory of Transformations in Metals and Alloys*, p. 830. Pergamon Press, Oxford (1965).
34. F. B. Pickering, *Transformation and Hardenability in Steels*, Symposium by the Climax Molybdenum Co., p. 109. Ann Arbor (1967).
35. K. R. Kinsman and H. I. Aaronson, Discussion to the paper of J. M. Oblak and R. F. Henemann, *Transformation and Hardenability in Steels*, p. 15. Symposium by the Climax Molybdenum Co., Ann Arbor (1967).

36. G. R. Srinivasan and C. M. Wayman, *Acta metall.* **16**, 621 (1968).
37. H. K. D. H. Bhadeshia, *Metal Sci.* in press.
38. H. K. D. H. Bhadeshia, Ph.D. Thesis, University of Cambridge, England (1979).
39. H. I. Aaronson, H. A. Domian and G. M. Pound, *Trans. metall. Soc. A.I.M.E.* **236**, 768 (1966).
40. B. Uhrenius, *Scand. J. metall.* **2**, 177 (1973).
41. H. K. D. H. Bhadeshia, *Metal Sci.* in press.
42. J. A. Lobo and G. H. Geiger, *Metall. Trans A* **7**, 1359 (1976).
43. H. K. D. H. Bhadeshia, *Metal Sci.* **14**, 230 (1980).

APPENDIX I

DETAILS ON THE THERMODYNAMIC CALCULATIONS

The equation used to calculate $\Delta F^{\gamma-\gamma_1+\alpha}$ for Fe–C alloys was the same as equation (20) of [24], based on the Lacher, Fowler and Guggenheim theory. For this purpose, $x_\gamma^{\gamma\alpha}$ (Ae_3 composition) was calculated using equation (13) [24]. It should be noted that the latter contains a typographical error, so that all the x_γ terms should read $x_\gamma^{\gamma\alpha}$.

For alloy steels, the above equations were modified as in [35, 39]. The influence of alloying elements on the carbon–carbon interaction energy in austenite was derived from the optimised activity data of Uhrenius [40], using the methods of [39]. The full details are given in [41]. The partial molar enthalpies and excess partial molar entropies of solution of carbon in austenite and ferrite were obtained from [25, 42].

$\Delta F^{\gamma-\alpha_s}$ was calculated as in [37], but the relevant equation is also published in [30]. For this purpose, the carbon–carbon interaction energy in ferrite was taken to be the average of the values listed in [43]. Zener ordering was taken into account in these calculations.